Available online at www.sciencedirect.com

SciVerse ScienceDirect

journal homepage: www.elsevier.com/locate/issn/15375110

Research Paper

Plant leaf detection using modified active shape models

Chunlei Xia [a,b,e], Jang-Myung Lee [a], Yan Li [a], Yoo-Han Song [c], Bu-Keun Chung [d], Tae-Soo Chon [b,*]

[a] School of Electrical Engineering, Pusan National University, Busan (Pusan) 609-735, Republic of Korea
[b] Department of Biological Sciences, Pusan National University, Busan (Pusan) 609-735, Republic of Korea
[c] Department of Applied Biological and Environmental Science, Gyeongsang National University, Jinju, Republic of Korea
[d] Division of Plant Environment, Gyeongnam Agricultural Research and Extension Services, Jinju, Republic of Korea
[e] Yantai Institute of Coastal Zone Research, Chinese Academy of Sciences, Yantai 264003, PR China

ARTICLE INFO

Article history:
Received 9 October 2012
Received in revised form
29 April 2013
Accepted 7 June 2013
Published online 14 July 2013

We propose an *in situ* detection method of multiple leaves with overlapping and occlusion in greenhouse conditions. Initially a multilayer perceptron (MLP) is used to classify partial boundary images of pepper leaves. After the partial leaf boundary detection, active shape models (ASMs) are subsequently built to employ the images of entire leaves based on *a priori* knowledge using landmark. Two deformable models were developed with pepper leaves: Boundary-ASM and MLP-ASM. Matching processes are carried out by deforming the trained leaf models to fit real leaf images collected in the greenhouse. MLP-ASM detected 76.7 and 87.8% of overlapping and occluded pepper leaves respectively, while Boundary-ASM showed detection rates of 63.4 and 76.7%. The detection rates by the conventional ASM were 23.3 and 29.3%. The leaf models trained with pepper leaves were further tested with leaves of paprika, in the same family but with more complex shapes (e.g., holes and rolling). Although the overall detection rates were somewhat lower than those for pepper, the rates for the occluded and overlapping leaves of paprika were still higher with MLP-ASM (ranging from 60.4 to 76.7%) and Boundary-ASM (ranging from 50.5 to 63.3%) than using the conventional active shape model (from 21.6 to 30.0%). The modified active shape models with the boundary classifier could be an efficient means for detecting multiple leaves in field conditions.

1. Introduction

In conventional farming, agricultural cultivation and pest management are conducted manually by farmers, causing human health problems and productivity loss. Recently, precision agriculture has been proposed to reduce the chemical stress to humans and agricultural products, relying on new technologies (Zhang, Wang, & Wang, 2002), such as computer vision and robotics.

Proper judgement of leaf status is essential for effective management of crops including cultivation and crop protection. Automatic detection of individual leaves is a fundamental

* *Corresponding author*. Tel.: +82 51 5102261; fax: +82 51 5812962.
E-mail address: tschon@pusan.ac.kr (T.-S. Chon).
1537-5110/$ – see front matter
http://dx.doi.org/10.1016/j.biosystemseng.2013.06.003

Nomenclature

ASM	Active shape model
b	Vector of weights
CPU	Central processing unit
D_m	Mahalanobis distance
G_{rgb}	Gray level value
kNN	k-nearest neighbour
l	Length from leaf centroid to boundary
MLP	Multilayer perceptron
n	Number of landmark points
N	Number of training images
p	Control point of Bezier curve
p_c	Centroid of leaf
P	Matrix of first t eigenvectors
PC	Personal computer
RAM	Random access memory
RGB	Red, Green and Blue
ROC	Receiver operating characteristic
S_m	Covariance matrix of pixels
t	Number of eigenvectors
T	Transpose operator
$\overline{X}$	Mean shape
x_i	ith shape in the training set
$x_{i,j}$,	x coordinate of jth point in ith training shape
x_{rgb}	Pixel in the RGB space
$y_{i,j}$	y coordinate of jth point in ith training shape
α	Angle at control point p_1
β	Angle between leaf centroid and boundary
μ_m	Mean value of vegetation pixels

task for achieving precision in agricultural practices, such as micro-spray, de-leafing, and plant inspection. Leaf detection is also a crucial and challenging task for vision-guided agricultural robotics, for instance, in a weed control robot for automatic weed recognition and precision control (Slaughter, Giles, & Downey, 2008).

Plant leaves, however, contain complex information (e.g., colour, morphology, and texture) which vary with growth conditions and are consequently difficult to detect or identify. Since the 1980s, numerous studies on leaf segmentation have been conducted (Guyer et al., 1984), including recent development of genetic and watershed algorithms for leaf information extraction (Lee & Slaughter, 2004; Neto, Meyer, & Jones, 2006; Tang, Zhao, & Tao, 2009; Wang, Ding, & Fang, 2008; Wang, Huang, Du, Xu, & Heutte, 2008). In addition, spectral images and stereo vision techniques have been introduced to solve problems of leaf extraction and segmentation of overlapping leaves (Noble & Brown, 2008; Teng, Kuo, & Chen, 2011). However, the early methods were largely dependent on local image features since only partial information is usually available under complex field conditions (e.g., overlapping leaves and leaves hidden from cameras). Considering both the importance and difficulty in obtaining information from whole leaf images, global information processing at higher level image recognition should also be developed to detect entire leaves.

Integrated algorithms could be a candidate for combining partial images to produce global image processing. The accumulation of *a priori* knowledge about targets (leaves) would be an alternative to generation of global information. Manh, Rabatel, Assemat, and Aldon (2001) developed a deformable template to accumulate information on weed leaves on the basis of the tips of leaves, while De Meezo, Rabatel, and Fiorio (2003) reported another shape-guided approach for leaf segmentation. Recently, Active Shape Models (ASMs) have been introduced for identification and classification of weed species (Søgaard, 2005; Persson & Åstrand, 2008; Swain et al., 2011). An ASM is a deformable template model and has sufficient tolerance to match shape variations of the same objects using *a priori* knowledge, and is sufficiently robust to locate known objects in the presence of noise and occlusion (Cootes & Taylor, 1992; Cootes, Taylor, Cooper, & Graham, 1995). ASM has been effectively used in various fields including medical image analysis, face recognition, and leaf pose estimation (Hamarneh, Abugharbieh, & McInerney, 2004; Milborrow & Nicolls, 2008; Moeslund, Aagaard, & Lerch, 2005).

Previous studies on leaf detection, however, were mainly concerned with identification of individual leaves with simple shapes such as weed leaves (e.g., smooth boundaries, linear shape). In this study, modified ASMs were developed to detect more complex shapes of vegetable leaves such as pepper leaves. By using the deformable process of ASM, two schemes are proposed: 1) Boundary-ASM matching leaf boundaries in binary images, and 2) MLP-ASM combining ASM with Multilayer Perceptron (MLP) classifier in gray-scale images. In order to effectively match whole leaves using ASM, leaf boundaries were identified prior to the execution of ASM for detecting whole leaves. An artificial neural network, MLP, was utilised as a boundary classifier.

An overview of the leaf detection procedure is shown in Fig. 1. After background removal, image edges representing leaf boundaries and veins were segmented according to the Bezier curve fitting. MLP was subsequently utilised for identification of leaf boundaries on the basis of input data given by

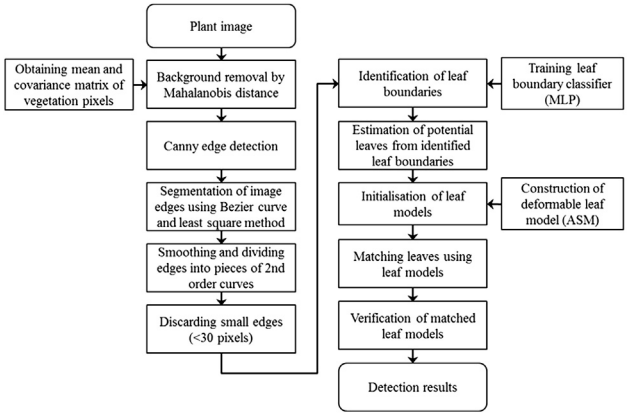

Fig. 1 – Overall procedure of learning and recognition of multiple leaves based on the deformable model and the boundary classifier.

the Bezier curves. Positions of hypothesised leaves were estimated from the leaf boundaries. Separately in line with leaf boundary identification, leaf models were developed to represent leaf shapes by accumulating information from the template leaf images obtained in a greenhouse. Subsequently, by integrating information on leaf shape defined by the partial leaf boundaries, the deformable model was produced to represent images of whole leaves.

The preparation of plant leaf images for this study is presented in Section 2, while the procedure for detecting multiple plant leaves is discussed in Section 3. Experimental results and discussion are given in Section 4 and 5, followed by conclusions in Section 6.

2. Materials

Plant images were captured from pepper, *Capsicum annuum* (Solanaceae) (data set 1) and paprika, *Capsicum annuum var. angulosum* (Solanaceae) (data set 2 and 3). We selected pepper plants with young leaves for the test (Fig. 1a). Paprika plants with old leaves (i.e., more complex image) (data set 2) and young paprika leaves (data set 3) were additionally chosen for further application of the trained model (Fig. 1b and c). Paprika and pepper leaves are similar in shape as they are from the same family (Solanaceae). However, paprika leaves in data set 2 were large and older (i.e., broader area and curved boundary), and showed abnormal shapes more frequently due to diseases (e.g. holes, rolling) in this study. In data set 3, more complex images were provided with overlapped paprika leaves with various poses.

For both plant leaves, colour images were taken using a Pentax digital camera with a resolution of 640 × 480 pixels. Images of the pepper plants were obtained under light conditions in the range of 4210–5950 lux in the greenhouse (Fig. 2a). This illumination condition was generally comparable to the light in the greenhouse in the afternoon (around 3–4 p.m.) on a clear day in early summer in the North Temperate Zone. The images were captured from above with the camera located approximately 30 cm above the highest leaves. Data set 1 contained 24 pepper images, and 3–6 detectable leaves were captured in each image. The pepper plants were cultivated for one month, and the length of the pepper leaves was in the range of 4–6 cm (154–290 pixels). In this study, the small size pepper leaves on the canopy (less than 3 cm) were not used as recognition targets for simplicity of ASM application. Twenty individual pepper leaves and their mirror images from data set 1 were chosen as the training set for deformable leaf models. Since plant leaf shape is regarded as symmetric, the model would be more accurate in describing shape variations if the leaf model is trained with mirror images. Plant leaves frequently bend to either left or right side in field conditions, and this will break symmetry. Using mirror images for deformable model, this type of leaf shape variation could be efficiently solved (Søgaard, 2005).

Prior to applying ASM, training was conducted using MLP as the leaf boundary classifier, as stated above. The input data were collected from 15 typical boundaries in 10 leaf images of pepper. Local image features obtained from 100 points on the leaf boundaries (boundary of single leaf, and boundary of overlapping and occluded leaves) and 100 points on the veins were chosen as input data for training.

The paprika plants in data set 2 were grown for six months in pots in the laboratory. The leaves were older giving a more complex image with abnormal shapes (e.g., wilted area with brown colour) compared to pepper leaves (Fig. 2b). Images of paprika were collected outdoors under illumination ranging between 3240 lux and 4030 lux. This condition was comparable to late afternoon (around 4–5 p.m.) on a cloudy day in spring in North Temperate Zone. These images were captured using the same technique as outlined above for pepper. Complexity in images (e.g., holes, rolling) was higher in paprika compared to pepper. In total, 26 paprika images were collected for testing with the trained ASM. A maximum of four leaves were captured in one plant image. The length of leaves imaged ranged from 8 to 14 cm (240–430 pixels).

In data set 3, images of young paprika plants were taken from the glasshouse. The paprika plants were cultivated for one and half months. Leaves with more complex poses were chosen for detection. Leaves were overlapping while a proportion of the leaves bent in the horizontal direction showing only side views (Fig. 2c). White paper board was placed behind the plants to simplify the background. Background simplification has been used commonly for greenhouse robots, e.g., strawberry picking (Hayashi et al., 2010). Images were captured around 1–2 p.m. on a clear day in spring in North Temperate Zone. Light condition ranged between 4240 lux and 5530 lux. Data set 3 contained 111 images of young paprika plants, and 3–10 detectable leaves were captured in each image. The length of the young paprika leaves was in the range of 6–13 cm (148–264 pixels). More detailed information on the leaves in these data sets is presented in the Results section.

3. Method

3.1. *Preprocessing of leaf images*

For leaf detection, image backgrounds were removed at the outset (Fig. 1) by applying Mahalanobis distance (D_m):

$$D_m = \sqrt{(x_{rgb} - \mu_m)^T S_m^{-1} (x_{rgb} - \mu_m)} \quad (1)$$

where μ_m and S_m represent the mean and covariance matrix of the sampled pixels, respectively, x_{rgb} is the vector of a pixel in the RGB space, and T denotes the transpose. Mahalanobis distance is efficient in the segmentation of vegetation pixels from natural backgrounds against light changes in a certain range (Manh et al., 2001). The optimal threshold for segmentation of vegetation pixels was determined after testing various images, 10 for pepper, 40 for old paprika and 7 for young paprika. Additional noise in the background was further removed by applying erode-dilation operations. Contours of vegetation areas in the binary image were smoothed using morphological processes such as opening and closing (Gonzalez, Woods, & Eddins, 2004). Figure 3 shows the background-removed leaf images of Fig. 2. During the segmentation process, the old paprika leaf (Fig. 3b) lost much information when compared with pepper leaves (Fig. 3), since biological (e.g., disease in grey

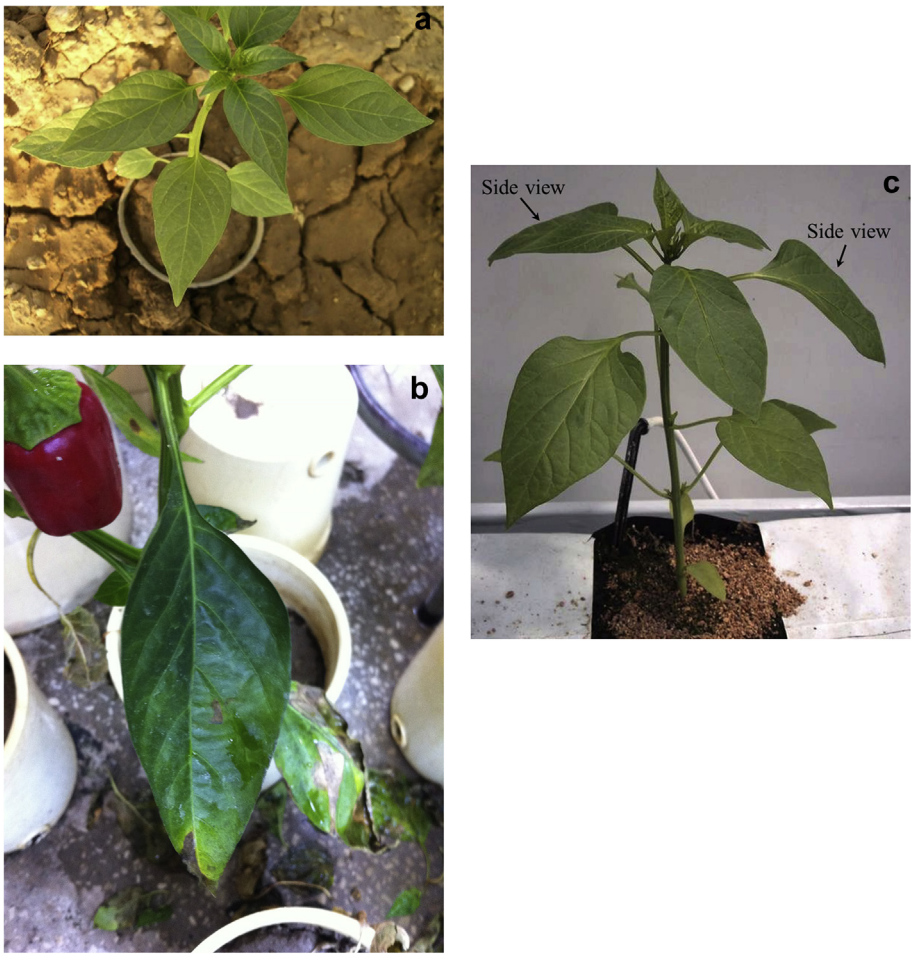

Fig. 2 – Captured plant images of (a) pepper, (b) old paprika and (c) young paprika.

colour) and natural (e.g., slight light reflections from the leaf) disturbances were prevalent on the old paprika leaf surface.

Subsequently, the Canny edge detection was used to determine image edges (Canny, 1987). The quadratic Bezier curve was initially applied to segmenting image edges into partial leaf boundaries. In the segmentation process, the Bezier curve was fitted to image edges by using the least square method (Shao & Zhou, 1996). The image edge was broken down into partial leaf boundaries at the points where fitting error was larger than a tolerance value. Fitting error was the distance between image edge and the fitted curve, and the maximal allowed fitting error in this study was determined as 20 pixels in order to achieve maximum efficiency of boundary segmentation from the preliminary tests. Although the cubic Bezier curves may be sensitive for detecting highly bent curves, we adopted the quadratic Bezier curves in this study. Due to high flexibility of the cubic Bezier curves in detecting curves, the boundaries of two overlapped leaves were frequently over-fitted as one continuous edge by cubic Bezier curves in pre-tests although two separate boundaries should have been. The quadratic Bezier was more stable in separating edges from two leaves in natural conditions.

After application of the Bezier curves, edges in the background-removed image of pepper leaves (Fig. 3a) were accordingly identified, as shown in Fig. 4. Extremely short edges with minimal distance (e.g., 30 pixels) were additionally observed due to aggregated noise spots. These spots were not regarded as leaf features in this study. According to the preliminary results, small edges were abnormally produced when the length was equal to or less than 30 pixels. This length was therefore used as a criterion for determining effective curves for leaf detection in this study.

3.2. *Leaf boundary classification*

Three types of edges in leaf images were defined in this study: vein, boundary of single leaf, and boundary of overlapping (and occluded) leaf. Leaf veins are located inside a leaf as an interior leaf boundary and tend to show similar tones in colour across the vein (Fig. 5a). The veins with strong edges may be sometimes confused with the boundaries of overlapping leaves. The boundaries of overlapping (and occluded) leaves, however, were substantially distinctive compared to veins, due to differences in light reflection and leaf status (e.g., maturity) (Fig. 5b). The boundary of a single leaf is defined as the boundary observed between the leaf and its background, which is relatively easier to detect in comparison to the veins and occluded/overlapping boundaries.

Images were converted to gray values according to Eq. (2) for extracting leaf features.

Fig. 3 – Background-removed leaf image. (a) Pepper, (b) old paprika and (c) young paprika.

$$G_{rgb} = 0.299R + 0.587G + 0.114B \quad (2)$$

where R, G and B represent the pixel values for the red, green and blue channels of the colour image, respectively (Gonzalez et al., 2004).

MLP was utilised for differentiating leaf boundaries from veins. The image feature, obtained from a sample line intersecting the edge perpendicularly, was used to present the local information surrounding the edge point. An example of obtaining local features from an overlapping leaf boundary is shown in Fig. 6. A straight line was drawn, crossing the edge along the gradient direction perpendicularly. The sample line consisted of 3 pixels on either side of the edge in addition to the centre point (i.e., profile of 7-pixels). Cootes and Taylor (1993) reported that a profile of 7 pixels was better than 3 or 5 pixels to locate image edges effectively. The profile of 7 pixels was sufficiently long to distinguish the image patterns across the leaf boundary and veins in the sampled data in this study. The sampled data (i.e., vectors for gray values) were transformed to the feature vectors (normalised in [0, 1]) and were used as the input data for training MLP (see Section 2).

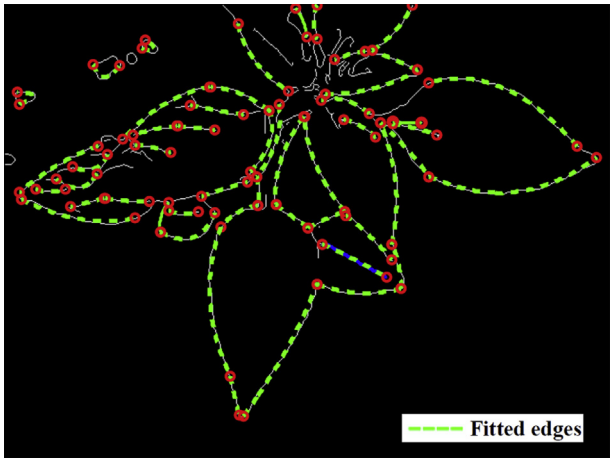

Fig. 4 – Edge images presented by the Bezier curves.

The MLP network consisted of three layers: seven nodes for the input layer, eight nodes for the hidden layer, and one node for the output layer. A typical structure for an MLP contains 3 layers, input vector and desired output (Rajab, Woolfson, & Morga, 2004). In the hidden layer, we adopted 8 nodes, since 8–10 nodes have been reported to produce superior performance for identification of edges from images with similar complexity to those used in this study (Zwaag & Slump, 2002). The output node of MLP was defined as a binary number: 1 for a leaf boundary and −1 for a leaf vein. In this study, two types of boundary (of single leaves and of overlapping/occluded leaves) were considered equivalent for identification, since the vectors of their images were practically the same after normalisation. The learning rate after training was 99.2%.

When more than 60% of the edge pixels were identified to belong to leaf boundary pixels, the edge was classified as a leaf boundary. The identified leaf boundaries of the pepper leaf image are shown in Fig. 7. Veins inside the leaves were

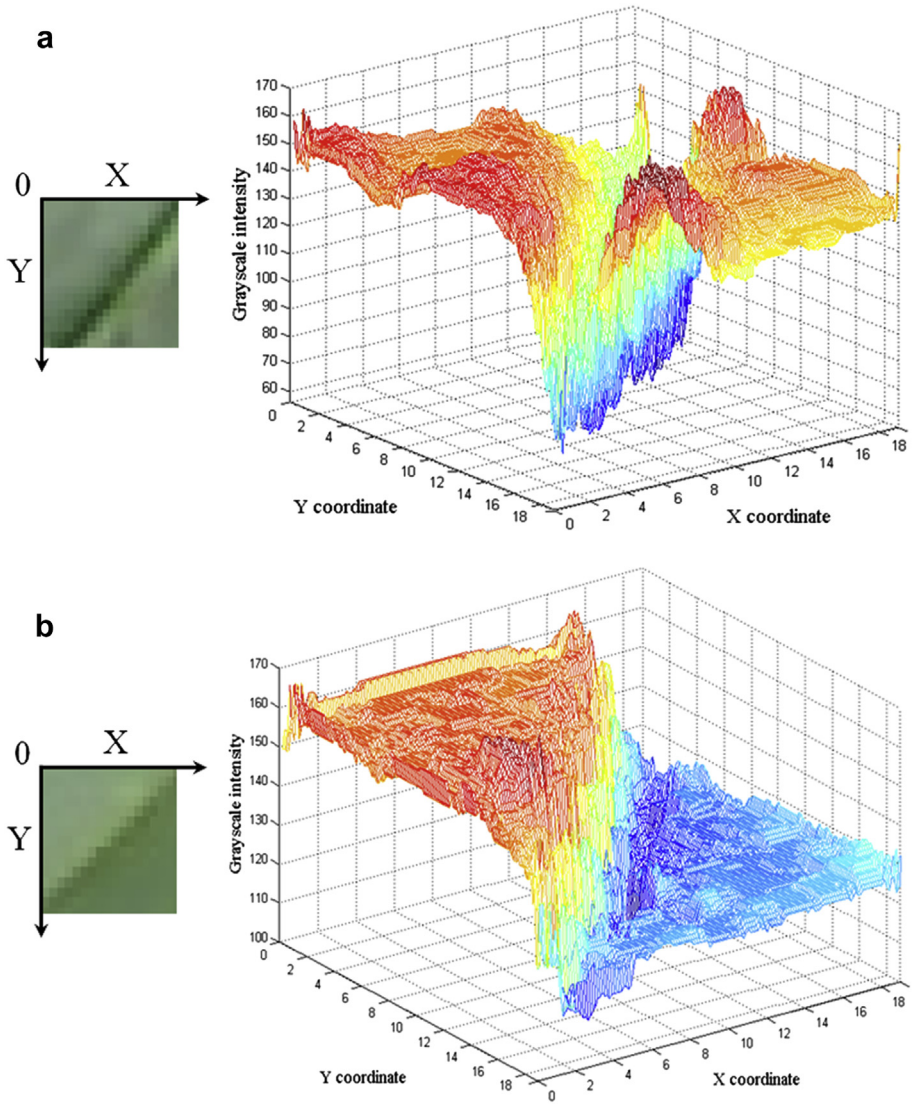

Fig. 5 – Local feature of (a) leaf vein and (b) boundary of overlapping leaves in different intensities. The insets are 2D projections of the area around the vein (a) and leaf boundary (b).

removed, and edges on the outskirts of leaves were connected to produce the boundary line.

3.3. *Building leaf-shape models*

In ASM, an object's shape is represented by a shape vector x_i with n landmarks:

$$\mathbf{x}_i = \left(x_{i,0}, y_{i,0}, x_{i,1}, y_{i,1}, \cdots, x_{i,n-1}, y_{i,n-1}\right)^T, i = 1, \cdots, N \quad (3)$$

where $(x_{i,j},y_{i,j})$ are the coordinates of the jth landmark of the ith shape in the training sets, N is the number of images in the training set, and T is the transpose operator. To build a deformable leaf model, typical leaves were selected and the sample leaves were manually marked with landmarks along their contours (Fig. 8). The optimal number of landmarks was determined according to preliminary tests. A small number of landmarks may not be sufficient to accurately represent leaf shape variation, whereas a large number of landmarks will cause unnecessary computational complexity and computation cost. Considering both leaf shape complexity and work demand for manual landmarking, 39 points in total was chosen to represent the leaf shapes in this work. The starting point of the leaf shape was the 1st point near the leaf petiole, the 20th point corresponded to its tip, and the shape was completed at the 39th point returning to the leaf petiole (Fig. 8). The sequence and position of landmarks were kept consistent throughout the training.

Before analysing shape variations, the leaf images were aligned by translating, rotating, and scaling to minimise the weighted squared distance between the corresponding points in the training set (Cootes, Taylor, Cooper, & Graham, 1995). After training, any shape in the training set could be represented approximately by the mean shape and weighted modes of variations:

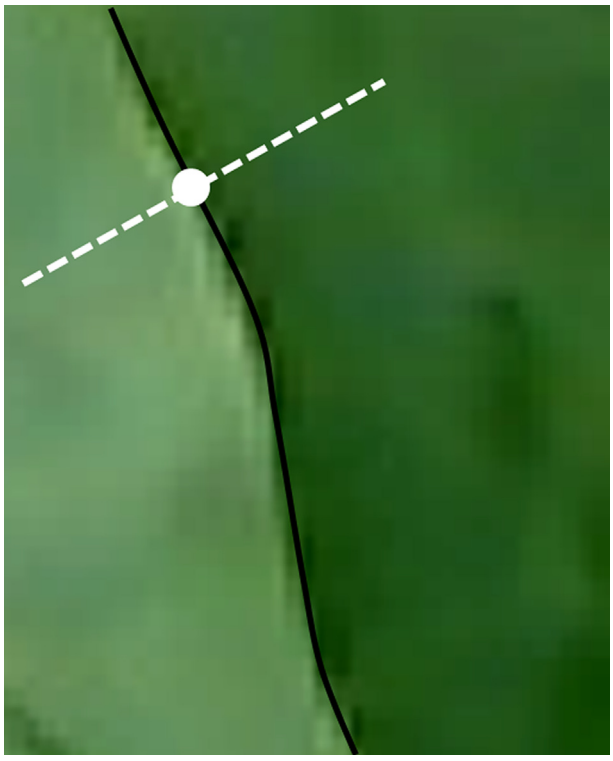

Fig. 6 – Feature vector of overlapping leaf boundary.

Fig. 8 – A leaf image in training set marked with landmarks.

$$\mathbf{x}_i = \overline{\mathbf{x}} + \mathbf{Pb} \quad (4)$$

where $P = [p_1, p_2, \ldots, p_t]$ is the matrix of the first t eigenvectors and b is the vector for weights. The model could be deformed from the mean (i.e., $\overline{\mathbf{x}}$) shape to fit the new data by changing the weight vector b (see Cootes et al. (1995) for detailed algorithms). In this study, the ASMs were implemented with Hamarneh's ASM code (Hamarneh, Abu-Gharbieh, & Gustavsson, 1998) under MATLAB 9.0 in PC (Intel Core 2 T7200 CPU and 3G RAM).

3.4. *Locating approximate leaf positions*

In order to match the model with the whole leaf image from field conditions, the template leaf was positioned near the field leaf image initially. The partial boundaries categorised according to the Bezier curves were used for finding the centre position of the leaf model. We divided the leaf boundary into two different types based on their curvature, as shown in Fig. 9. Type A consists of boundaries near the tip of the leaf. The shape of these boundaries approximates a straight line. Type B, on the other hand, consists of the curved boundary along the middle portion of the leaf edge.

Control points on the Bezier curve were used to describe the features of the curves. For the leaf edge at the side, for instance, the angle α at the control point p_1 was defined to describe the curvature of the boundary while the curve length was approximated by the length of line p_0p_2 (Fig. 9). Table 1 lists the rules for determining the edge types.

After the centre points were defined, the models were accordingly aligned near the field leaf image. In determining

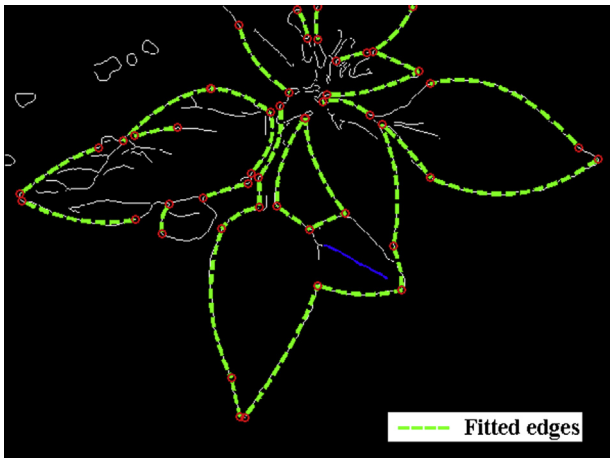

Fig. 7 – Identified leaf boundaries based on MLP.

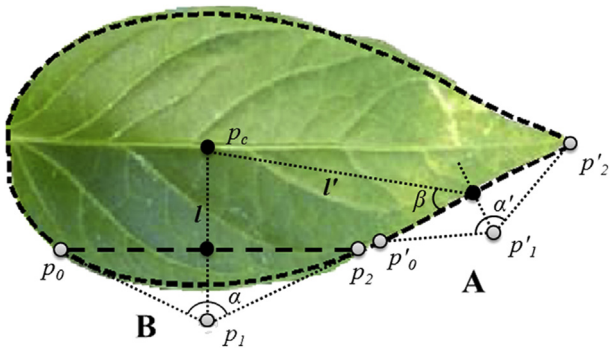

Fig. 9 – Definition of partial edge types and approximate centroid of a leaf: A is tip region, and B is side boundary.

Table 1 – Curvature, length and edge types defined in leaf boundaries.

	Lower edge		Middle edge	
Curvature	$170 < \alpha < 180$		$90 < \alpha < 170$	
Length	Short	Long	Short	Long
Edge type	A	B	B	B

the initial position of the model, the approximate centre point p_c of the model was estimated near the leaf image. The centre of the model was calculated in accordance from the geometric relationship between the centre of the leaf and its edges for both types A and B (Fig. 9). For type B, a centre point p_c was determined from a line with length l, which intersected line p_0p_1 perpendicularly. A predetermined distance ($l = 30$ pixels) was given as the length of a line to p_c, inward from p_1 to the centre of the leaf. For type A, the centre of the leaf was similarly estimated by the predefined length ($l' = 50$ pixels) and angle β (30°). These parameters (l, l' and β) were measured from the mean shape of leaves from the training set in this study. Although the centre of the leaf approximated in this way may not be a precise match with the actual centre point of the leaf, it was sufficiently close to the field images to start the deformation process.

3.5. *Deformable matching*

After initialisation, the leaf models search iteratively for the best matching leaf boundaries by translating, rotating, and scaling the shapes given in the training data sets. The approximate shapes of a leaf could be assumed according to aligning the position of the partial leaf boundaries. This process is somewhat similar to the recognition process by human beings (i.e., gestalt images): an overall object is perceived by associating partial features known *a priori* (Biederman, 1987). The weight vector b in Eq. (3) was adjusted accordingly when the model was deformed to fit the leaf images obtained under field conditions.

As illustrated in Fig. 10, the deforming processes were repeated to match image data until the model converged to the optimal position or the maximal step was reached as follows (Cootes *et al.*, 1995):

(1) For each landmark on the shape contour, the model finds the optimal locations along the normal to the landmark. The model searches best matching locations (i.e., leaf boundaries) of the image around each landmark and calculates the displacement from the current point to the preferred location.
(2) According to the displacement obtained in step (1), the optimal shape is adjusted by translation, rotation, scale and variation in parameters (i.e., weight vector b).
(3) The variation and location parameters of the model are updated.

In preliminary tests for leaf detection, we found that conventional ASM based on the Mahalanobis distance for feature matching could not effectively distinguish leaf boundaries especially from veins (Cootes et al., 1995). Therefore, we devised two new processes to solve this problem in this study (Table 2). Firstly, we proposed a method called Boundary-ASM to match classified leaf boundaries only (not including veins) using the MLP classifier (Fig. 7). This method is relatively simple as it uses a binary image to carry out the matching process. However, in this method, part of the boundary information may be missed during the matching process, since small discontinuous boundaries are considered as noise on the leaf boundary. Secondly, we devised the MLP-ASM method. This method uses the information on both sides of the edge, along with the line perpendicular to the curves where the landmarks are located (Fig. 8). The proposed leaf boundary classifier (see Section 3.2) was also incorporated with the MLP-ASM method for the matching processes. The MLP classifier examines each pixel along the search path at each landmark and identifies the boundary pixels for deformation (Fig. 11). The search radius and the maximal step were both estimated from preliminary studies. Performance of leaf detection was conducted across different levels of search radius and maximal step. The search radius was adjusted to 30 pixels for both upward and downward directions at each landmark. A small search radius made it difficult for the model to find the leaf boundary, whereas with a large radius the model results would reduce the matching accuracy in addition to increasing the computation cost. The maximal step of matching was set to 100.

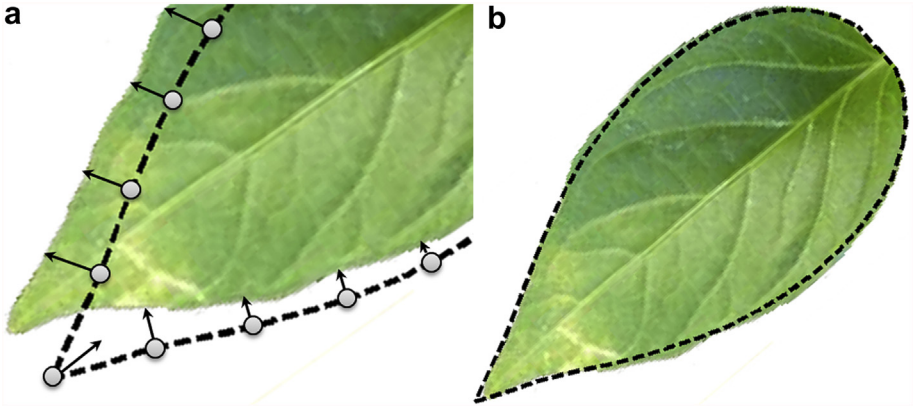

Fig. 10 – Searching and convergence of leaf images using the deformable models. (a) Process of searching optimal points, and (b) the leaf model converged to image data.

Table 2 – Comparison of leaf recognition methods in ASM, Boundary-ASM and MLP-ASM

	ASM	Boundary-ASM	MLP-ASM
Image data	Gray	Binary	Gray
Image feature	1D gradient profile	1D binary data	Local image feature (1D)
Feature matching function	Mahalanobis distance	Finding binary leaf boundary	Leaf boundary classifier
Identification of leaf boundaries	No	Yes	Yes

4. Results

Classification of leaf boundaries using MLP was conducted prior to detection of the whole leaf by ASM (Table 3). Images of pepper (24 images with 105 leaves) were tested by the trained MLP for leaf boundary classification (Section 3.2). The testing data contained 2181 edges (length of the edges: 30–120 pixels) with 1024 leaf boundaries and 1157 veins. The classification rate was in the acceptable range of 87.1% for a leaf boundary and 97.1% for a non-leaf boundary (vein) for pepper (Table 3).

After leaf boundary classification, multiple leaf detection was carried out using the proposed ASMs on pepper leaves in data set 1 (Sections 3.3–3.5). An example image is shown in Fig. 12(a), where six pepper leaves in various poses and shapes (single, overlapping, and occluded) were successfully detected. Table 4 summarises the detection rates for pepper leaves. Detection rates for single leaves were 85.7%, for the conventional and proposed ASMs. Detection rates for overlapping and occluded leaves, however, were remarkably high using the MLP-ASM method (87.8%) followed by the Boundary-ASM method (63.4%) in contrast to detection rates for the conventional ASM (23.3–29.3%) (Table 4).

The leaf model trained with pepper leaves was further tested on paprika which have more complexity in shape (Tables 5 and 6). In data set 2 for paprika, few single leaves were available for testing since the plant was mature at the time of the experiment, and most of the leaves were ill-formed and overlapped with other leaves and stems. The leaves with severe deformation (e.g., deep wilt) were not used for detection in this study. Nine single leaves were available for testing (Table 5). Prior to ASM, leaf boundary classification was initially conducted by testing 2186 edges (860 leaf boundaries and 1326 veins) obtained from 26

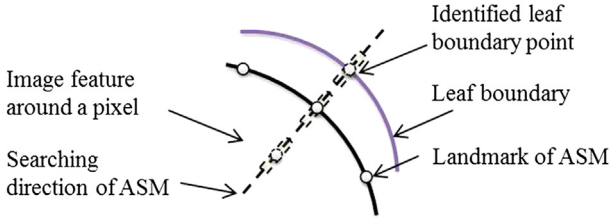

Fig. 11 – Searching process of leaf image by examining local feature along the perpendicular line crossing the landmark.

Table 3 – Classification rates (%) of leaf boundaries and veins of pepper and paprika by the trained MLP.

Edge type	Pepper		Paprika	
	Classification (%)	Number of edges	Classification (%)	Number of edges
Leaf boundary	87.1	1024	85.1	860
Vein	97.1	1157	96.4	1326

paprika images. The boundaries were classified accordingly at a rate between 85.1% and 96.4% (Table 3). Fig. 12(b) presents one of the detection results on the old paprika images in data set 2. This detection result was carried out with the background-removed image (Fig. 3b): the diseased and reflection areas were removed with the background, forming holes and disconnected boundaries on the leaf. Boundary-ASM performed at the same level as the conventional ASM when detecting single old paprika leaves, while MLP-ASM performed better. When detecting overlapping and occluded leaves, the detection rates were remarkably improved using MLP-ASM (70.0–76.7%) or Boundary-ASM (60.0–63.3%) compared to the conventional ASM (25.0–30.0%) (Table 5).

For leaf detection with young paprika leaves in data set 3, the leaves were posed in various directions, with the leaves in Fig. 12c showing front and side views. The small leaves (<3 cm) on top of the canopy were excluded from the detection since they were clustered too closely and could not present necessary features (boundaries) for detection. In total, 577 leaves, including 187 single leaves, 279 overlapping leaves and 111 occluded leaves, were tested. As presented in Table 6, detection rate was 78.6% for single leaves with MLP-ASM, and was 71.1% and 47.1% with Boundary-ASM and the conventional ASM respectively. Performance when detecting overlapping leaves was comparable to MLP-ASM (71.0%) and Boundary-ASM (66.3%), however, the conventional ASM was substantially lower at 21.9%. The proposed MLP-ASM also showed the highest detection rate (60.4%) for occluded leaves comparing with the proposed Boundary-ASM (50.5%) and the conventional ASM (21.6%). The overall detection rate of MLP-ASM (71.2%) was superior to Boundary-ASM (64.8%) and the conventional ASM (30.0%). The detection rates of Boundary-ASM and MLP-ASM are significantly higher than conventional ASM according to multiple comparison test (Tables 4–6) (Zar, 1999, chap. 11).

Receiver operating characteristic (ROC) was further utilised to evaluate performance of the proposed methods (Fawcett, 2006) (Table 7). ROC is a graphic tool to illustrate the performance of a classification system by matching true/false results between models and experiments. We defined “true positive” as correct detection of an actual leaf image by a leaf model. If the model reports a leaf on a non-leaf image area, this would be “false positive”. On the contrary, if no leaf is detected on a non-leaf area by the model, the result will be called “true negative”, whereas “false negative” indicates that the detection of leaf was failed in the leaf image area. True positive rate (TRP) and false positive rate (FPR) were the criteria used in ROC plots in this study:

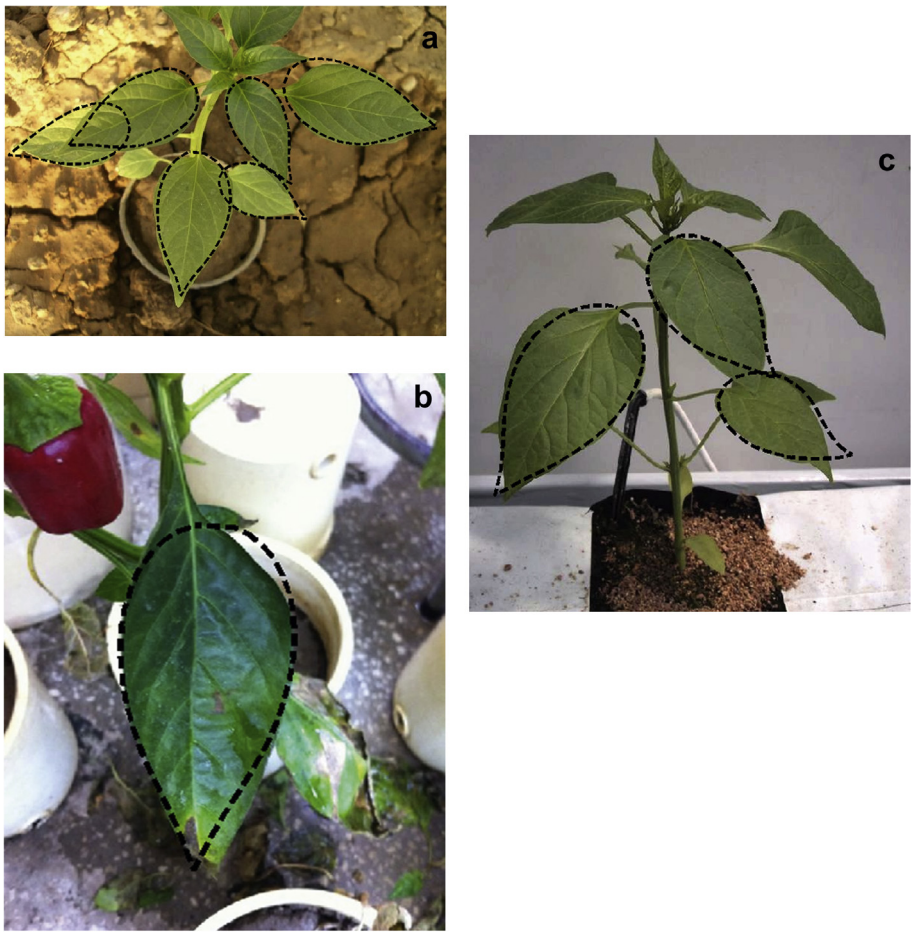

Fig. 12 – Detection of (a) pepper leaves, (b) old paprika leaves with disease and (c) young paprika leaves by using MLP-ASM.

$$TPR = \frac{\text{True Positive}}{\text{True Positve} + \text{False Negative}}, \quad (5)$$

$$FPR = \frac{\text{False Positive}}{\text{False Positve} + \text{True Negative}}. \quad (6)$$

A total of 105 pepper leaves (data set 1) were examined using 648 deformable models for pepper, 824 models from 59 leaves for old paprika in data set 2 and 2421 models from 577 leaves for young paprika in data set 3. True positive rates were substantially different among the proposed models, while false positive rates were quite similar among the different methods. The performance of MLP-ASM was best, followed by Boundary-ASM and ASM for both pepper and paprika.

Overall, performance of the proposed model was remarkably better, especially in detecting complex leaf shapes. The occluded pepper leaves were recognised by MLP-ASM at 87.8% compared with the original ASM at 25.0% (Table 4). The leaves

Table 4 – Detection rates (%) based on ASM, boundary-ASM and MLP-ASM for single, overlapping or occluded leaves of pepper. a, b indicating statistical significance (Tukey HSD, $p < 0.05$).

	Detection rates (%) and no. of detected leaves			No. of leaves
	ASM	Boundary-ASM	MLP-ASM	
Single leaves	85.7% (18)[a]	85.7% (18)[a]	85.7% (18)[a]	21
Overlapping leaves	23.3% (10)[a]	76.7% (33)[b]	76.7% (33)[b]	43
Occluded leaves	29.3% (12)[a]	63.4% (26)[b]	87.8% (36)[b]	41
Average	46.1%	75.3%	83.4%	

Table 5 – Detection rates (%) based on ASM, boundary-ASM and MLP-ASM for single, overlapping or occluded leaves of old paprika. a, b indicating statistical significance (Tukey HSD, $p < 0.05$).

	Detection rates (%) and no. of detected leaves			No. of leaves
	ASM	Boundary-ASM	MLP-ASM	
Single leaves	66.7% (6)[a]	66.7% (6)[a]	77.8% (7)[a]	9
Overlapping leaves	30.0% (9)[a]	63.3% (19)[b]	76.7% (23)[b]	30
Occluded leaves	25.0% (5)[a]	60.0% (12)[b]	70.0% (14)[b]	20
Average	40.6%	63.3%	74.8%	

Table 6 – Detection rates (%) based on ASM, boundary-ASM and MLP-ASM for single, overlapping or occluded leaves of young paprika. a, b indicating statistical significance (Tukey HSD, $p < 0.05$).

	Detection rates (%) and no. of detected leaves			No. of leaves
	ASM	Boundary-ASM	MLP-ASM	
Single leaves	47.1% (88)[a]	71.1% (133)[b]	78.6% (147)[b]	187
Overlapping leaves	21.9% (61)[a]	66.3% (185)[b]	71.0% (198)[b]	279
Occluded leaves	21.6% (24)[a]	50.5% (56)[b]	60.4% (67)[b]	111
Average	30.0%	64.8%	71.2%	

with higher complexity (e.g., holes, broken boundaries) were still detectable using the proposed ASMs (Figs. 3b and 12b). The improved ASMs could be further applied to paprika (Tables 5 and 6). The detection rates were comparable to pepper. This feasibility of the proposed ASMs could provide a flexibility of application to varieties of plants within the same taxa.

5. Discussion

One reason for high detection rates may be the flexibility of the multiple model generation in detecting diverse shapes of leaves. Since the presence of a leaf could be assumed from various partial leaf boundaries, numerous leaf models could be generated for matching the target leaf image. Among the multiple candidates, the model showing the best fit (i.e., the model with the largest area) could be chosen for the target leaf in a flexible manner. Another reason for the high recognition rate by the proposed methods may be the accuracy of locating the leaf boundary using the MLP. The MLP presented high rates for detecting leaf boundaries from leaf veins (Table 2).

In addition to deformable matching of leaf shapes, we also demonstrated the feasibility of using neural networks to identify boundaries of leaves in this study, being superior to the criterion based on Mahalanobis distance. Mahalanobis distance has been conventionally employed by the ASM for matching local leaf features (Cootes, Taylor, Cooper, & Graham, 1995). However, Mahalanobis distance showed lower accuracy in pattern recognition in practice, compared to application of neural network (Shaffer, Rose-Pehrsson, & McGill, 1999). This may be due to the fact that Mahalanobis distance depends on the covariance matrix obtained from the training samples and is only efficient in segmentation of vegetation pixels in a limited range in colour against light changes (Manh *et al.*, 2001). When image feature shows a wide range variance in colour patterns from the training samples, the Mahalanobis distance would lose the accuracy of feature matching. In addition, since only single leaves were contained in the training samples, boundary features of overlapped or occluded leaves were not modelled by Mahalanobis distance in the conventional ASM. Consequently, the conventional ASM was limited in comprehending overall image shapes in this study, especially for overlapped or occluded leaves. In contrast, the neural network was trained with all types of leaf boundaries, and was capable of extracting information from nonlinear data, such as boundary of overlapping and occluded leaves, as demonstrated with the field data in our research.

Table 7 – ROC analysis of leaf recognition by the original and proposed ASMs on pepper leaves, old paprika leaves and young paprika leaves.

Data sets	Methods	TPR	FPR
Pepper leaves	MLP-ASM	0.834	0.035
	Boundary-ASM	0.753	0.037
	ASM	0.461	0.016
Old paprika leaves	MLP-ASM	0.748	0.021
	Boundary-ASM	0.633	0.024
	ASM	0.406	0.012
Young paprika leaves	MLP-ASM	0.712	0.024
	Boundary-ASM	0.648	0.029
	ASM	0.300	0.003

Although the proposed models were outstanding in detecting the leaves in greenhouse conditions, there were problems to be considered, regarding minimisation of various noise sources on the leaf image *in situ*. By handling noise efficiently, there would be a possibility that "false positive" results could be decreased. The leaf posture and backgrounds of the plants were highly complex in the greenhouse. False positives are usually caused by the area of leaf veins that are mistaken for leaf boundaries, or from abnormal convergence of the model on the leaves. False positives occurred in detection of leaves at rates of 3.5%, 3.7%, and 1.6% for MLP-ASM, Boundary-ASM, and ASM, respectively, for field images of peppers (data set 1). For old paprika (data set 2) and young paprika leaves (data set 3), false positives were still similarly observed as 2.1% (MLP-ASM), 2.4% (Boundary-ASM), 1.2 (ASM) and 2.4% (MLP-ASM), 2.9% (Boundary-ASM), 0.3% (ASM), respectively.

Due to insufficient leaf coverage by ASM, incorrect matching was also experienced, especially in larger leaves with length >6 cm (250 pixels) for data set 1, length >13 cm (400 pixels) for data set 2 and length >12 cm (260 pixels) for data set 3. Coverage of the occluded leaf was occasionally less than 40% of the leaf surface. The deformed model usually required 40–70% of the actual leaf images. According to the author's experience, a large proportion of vegetation area (more than 80%) in the model would be required to guarantee correct detection. Scales in model size would be another issue in improving the recognition rate in ASM. In this study, we assumed the leaves are of a similar size for recognition and only one scale of model was generated for detecting leaves instead of using multi-resolution search. For accurate detection, the model should be similar in size to the actual leaf (±10%). Multi-scale model generation would contribute to further improvement in recognition rate. Furthermore, the maximal acceptable angle between the matched leaf model and actual leaf should be within ±30°.

Additional refinement of the algorithm may include improvement of detection performance in complicated scenes in field conditions, covering tracing the boundary of overlapping and occluded leaves, optimising the alignment of ASM (Wang, Ding, et al., 2008; Wang, Huang, et al., 2008), and stable vegetation segmentation in realistic conditions (McCarthy, Hancock, & Raine, 2010). To improve the accuracy of matching the leaf boundary, especially for irregular shapes, the

optimal alignment of landmarks and increase in the number of landmarks may be further considered (Belcher & Du, 2009; Van Ginneken, Frangi, Staal, & ter Haar Romeny, 2002; Zhao, Gao, Shan, & Yin, 2004). Other criteria for future improvement of detection are coverage of image, size, and angle difference between actual and model leaves.

Another problematic issue is computational cost, especially with MLP-ASM. The run-times for matching a leaf (5–100 iterations) are 0.22–4.38 s with ASM, 0.05–1.08 s with Boundary-ASM and 4.05–81.46 s with MLP-ASM. The MLP classifier appears to be most computationally expensive. However, a comparable algorithm, the precise feature matching function (e.g., kNN), for instance, also takes around 26 times longer than calculating Mahalanobis distance in the original ASM. MLP-ASM took around 20 times longer than the time for the original ASM on average (Van Ginneken *et al.*, 2002). Since agricultural practices (i.e., continuous, steady plant inspection) may not require extremely short time performance, the proposed methods could be still applied to practical situations in reasonable time scale. The run-time could be significantly reduced by implementing the algorithm in C++ (Swain et al., 2011). Further development may be needed to reduce calculation cost.

6. Conclusions

Detection of multiple leaves with overlapping and occlusion in field conditions (greenhouse) was successfully performed by modified models of ASM in cooperation with a leaf boundary classifier. While the neural network classifier was efficient in the selection and identification of leaf boundaries, the proposed ASMs were capable of producing overall leaf shapes in a flexible manner by integrating the partial leaf boundaries. Remarkable improvement in detection rates for the leaves with overlapping and occlusion was achieved in the MLP-ASM followed by the Boundary-ASM compared to the conventional ASM.

The proposed models were also effective in detecting leaves of other varieties within the same species, demonstrating feasibility in deformable shaping by the ASM. The proposed ASMs would be suitable for leaf detection *in situ* and could assist various agricultural practices, including micro-dosing spray, plant inspection, and warning of infected leaves.

Acknowledgements

This works was supported by Korea Institute of Planning and Evaluation for Technology of Food, Agriculture, Forestry, and Fisheries under grant number 108929033HD120.

REFERENCES

Belcher, C., & Du, Y. (2009). Region-based SIFT approach to iris recognition. *Optics and Lasers in Engineering, 47*(1), 139–147.

Biederman, I. (1987). Recognition-by-components: a theory of human image understanding. *Psychological Review, 94*, 115–147.

Canny, J. (1987). A computational approach to edge detection. In M. A. Fischler, & O. Firschein (Eds.), *Readings in computer vision: Issues, problems, principles, and paradigms* (pp. 184–203). San Francisco: Morgan Kaufmann Publishers.

Cootes, T. F., & Taylor, C. J. (1992). Active shape model – 'smart snakes'. In *Proceedings of British machine vision conference* (pp. 266–275). Leeds, UK: BMVA Press.

Cootes, T. F., & Taylor, C. J. (1993). Active shape model search using local grey-level models: a quantitative evaluation. In *Proceedings of British machine vision conference* (pp. 639–648). Guildford, UK: BMVA Press.

Cootes, T. F., Taylor, C. J., Cooper, D. H., & Graham, J. (1995). Active shape models-their training and application. *Computer Vision and Image Understanding, 61*(1), 38–59.

De Meezo, B., Rabatel, G., & Fiorio, C. (2003). Weed leaf recognition in complex natural scenes by model-guide edge pairing. In J. Stafford, & A. Werner (Eds.), *Precision agriculture* (pp. 141–147). The Netherlands: Wageningen Academic Publishers.

Fawcett, T. (2006). An introduction to ROC analysis. *Pattern Recognition Letters, 27*, 861–874.

Gonzalez, R. C., Woods, R. E., & Eddins, S. L. (2004). *Digital image processing using MATLAB*. India: Pearson Education (Chapter 6, 9).

Guyer, D. E., Miles, G. E., Schreiber, M. M., Mitchell, O. R., & Vanderbilt, V. C. (1984). Machine vision and image processing for plant identification. *Transaction of ASAE, 29*(6), 1500–1507.

Hamarneh, G., Abugharbieh, R., & McInerney, T. (2004). Medial profiles for modeling deformation and statistical analysis of shape and their use in medical image segmentation. *Image and Vision Computing, 22*(6), 461–470.

Hamarneh, G., Abu-Gharbieh, R., & Gustavsson, T. (1998). Review – active shape models – part I: modeling shape and gray level variation. In *Proceedings of Swedish symposium on image analysis* (pp. 125–128). Uppsala: Sweden.

Hayashi, S., Shigematsu, K., Yamamoto, S., Kobayashi, K., Kohno, Y., Kamata, J., & Kurita, M. (2010). Evaluation of a strawberry-harvesting robot in a field test. *Biosystems Engineering, 105*(2), 160–171.

Lee, W. S., & Slaughter, D. C. (2004). Recognition of partially occluded plant leaves using a modified watershed algorithm. *Transaction of ASAE, 47*(4), 1269–1280.

Manh, A.-G., Rabatel, G., Assemat, L., & Aldon, M.-J. (2001). Weed leaf image segmentation by deformable templates. *Journal of Agricultural Engineering Research, 80*(2), 139–146.

McCarthy, C. L., Hancock, N. H., & Raine, S. R. (2010). Applied machine vision of plants: a review with implications for field deployment in automated farming operations. *Intelligent Service Robotics, 3*(4), 209–217.

Milborrow, S., & Nicolls, F. (2008). Locating facial features with an extended active shape model. In *Proceedings of 10th European conference on computer vision* (pp. 504–514). Marseille, France: Springer.

Moeslund, T. B., Aagaard, M., & Lerche, D. (2005). 3D pose estimation of cactus leaves using an active shape model. In *Proceedings of 7th IEEE workshops on application of computer vision* (pp. 468–473). Breckenridge, USA: IEEE.

Neto, J., Meyer, G., & Jones, D. (2006). Individual leaf extractions from young canopy images using Gustafson-Kessel clustering and a genetic algorithm. *Computers and Electronics in Agriculture, 51*, 66–85.

Noble, S. D., & Brown, R. (2008). Spectral band selection and testing of edge-subtraction leaf segmentation. *Canadian Biosystems Engineering, 50*, 2.1–2.8.

Persson, M., & Åstrand, B. (2008). Classification of crops and weeds extracted by active shape models. *Biosystems Engineering, 100*(4), 484–497.

Rajab, M. I., Woolfson, M. S., & Morgan, S. P. (2004). Application of region-based segmentation and neural network edge

detection to skin lesions. *Computerized Medical Imaging and Graphics, 28*(1–2), 61–68.
Shaffer, R. E., Rose-Pehrsson, S. L., & McGill, R. A. (1999). A comparison study of chemical sensor array pattern recognition algorithms. *Analytica Chimica Acta, 384*(3), 305–317.
Shao, L., & Zhou, H. (1996). Curve fitting with Bezier cubics. *Graphical Models and Image Processing, 58*(23), 223–232.
Slaughter, D. C., Giles, D. K., & Downey, D. (2008). Autonomous robotic weed control systems: a review. *Computers and Electronics in Agriculture, 61*(1), 63–78.
Søgaard, H. T. (2005). Weed classification by active shape models. *Biosystems Engineering, 91*(3), 271–281.
Swain, K. C., Nørremark, M., Jørgensen, R. N., Midtiby, H. S., & Green, O. (2011). Weed identification using an automated active shape matching (AASM) technique. *Biosystems Engineering, 110*(4), 450–457.
Tang, X., Liu, M., Zhao, H., & Tao, W. (2009). Leaf extraction from complicated background. In *Proceedings of 2nd international congress on image and signal processing* (pp. 1–5). Tianjin, China: IEEE.
Teng, C. H., Kuo, Y. T., & Chen, Y. S. (2011). Leaf segmentation, classification, and three-dimensional recovery from a few images with close viewpoints. *Optical Engineering, 50*, 937–946.
Van Ginneken, B., Frangi, A. F., Staal, J. J., ter Haar Romeny, B. M., & Viergever, M. A. (2002). Active shape model segmentation with optimal features. *IEEE Transactions on Medical Imaging, 21*(8), 924–933.
Wang, L., Ding, X., & Fang, C. (2008). Generic face alignment using an improved active shape model. In *International conference on IEEE audio, language and image processing* (pp. 317–321). Shanghai, China: IEEE.
Wang, X., Huang, D., Du, J., Xu, H., & Heutte, L. (2008). Classification of plant leaf images with complicated background. *Applied Mathematics and Computation, 205*(2), 916–926.
Zar, J. H. (1999). *Biostatistical analysis* (4th ed.). New Jersey: Prentice Hall.
Zhang, N., Wang, M., & Wang, N. (2002). Precision agriculture – a worldwide overview. *Computers and Electronics in Agriculture, 36*(2–3), 113–132.
Zhao, S., Gao, W., Shan, S., & Yin, B. (2004). Enhance the alignment accuracy of active shape models using elastic graph matching. In *Proceedings of international conference on biometric authentication* (pp. 52–58). Hong Kong, China: Springer.
Zwaag van der, B. J., & Slump, C. H. (2002). Analysis of neural networks for edge detection. In *The 13th annual workshop on circuits, systems and signal processing* (pp. 580–586). Veldhoven, the Netherlands.